Inflammopharmacol (2018) 26:183–195
https://doi.org/10.1007/s10787-017-0374-8

Inflammopharmacology

ORIGINAL ARTICLE

Anti-inflammatory and antialgic actions of a nanoemulsion of *Rosmarinus officinalis* L. essential oil and a molecular docking study of its major chemical constituents

Raphaelle Sousa Borges[1,7] · Emerson Silva Lima[2] · Hady Keita[1,3] · Irlon Maciel Ferreira[1] · Caio Pinho Fernandes[4,7] · Rodrigo Alves Soares Cruz[4] · Jonatas Lobato Duarte[1] · Josué Velázquez-Moyado[5] · Brenda Lorena Sánchez Ortiz[1,7] · Andrés Navarrete Castro[5] · Jaderson Vieira Ferreira[6,7] · Lorane Izabel da Silva Hage-Melim[6,7] · José Carlos Tavares Carvalho[1,7]

Received: 13 June 2017 / Accepted: 6 July 2017 / Published online: 13 July 2017

Abstract We evaluate the anti-inflammatory and antialgic potency of a nanoemulsion (NEORO) containing the essential oil of *Rosmarinus officinalis* L. (EORO), which is composed primarily of limonene, camphor and 1,8-cineole. The EORO and NEORO were administered orally 30 min prior to starting the experiments. In a test of rat paw oedema induced by carrageenan, NEORO was effective in doses of 498 μg/kg, and it inhibited 46% of the maximum peak of the oedema; in a dose of 300 mg/kg, EORO inhibited 50% of the maximum peak of the oedema. In an acetic acid-induced writhing test, NEORO yielded a dose-dependent effect, and a dose of 830 μg/kg inhibited 84% of the algesic process; a dose of 100 mg/kg of EORO inhibited 55%. In an assay for H_2S production in rat stomachs, a dose of 498 μg/kg of NEORO inhibited H_2S production in all of the measurement phases, and a dose of 100 mg/kg EORO inhibited 60% and influenced the effect of the ethanol significantly, reducing the production of H_2S. We suggest that NEORO potentiated the effect of EORO, demonstrating effectiveness in doses 600 times lower than those applied with EORO. Among the major compounds of EORO, the camphor molecule exhibited the largest number of interactions with the therapeutic targets related to the inflammatory process, suggesting that it is responsible for EORO's anti-inflammatory and antialgic effects. This work paves the way for future investigations related to the therapeutic role of NEORO in the inflammation process.

Keywords *Rosmarinus officinalis* · Nanoemulsions · H_2S · Anti-inflammatory · Antialgic · Molecular docking

✉ Raphaelle Sousa Borges
raphaellebio@yahoo.com.br

[1] Laboratório de Pesquisa em Fármacos, Departamento de Ciências Biológicas e Saúde, Universidade Federal do Amapá (UNIFAP), Rodovia Juscelino Kubitschek, S/N, Campus Marco Zero, Macapá, AP CEP 68903-419, Brazil

[2] Laboratório de Atividade Biológica – BIOPHAR, Universidade Federal do Amazonas, Avenida General Rodrigo Otávio, 6200 - Coroado I, Manaus, AM 69067-005, Brazil

[3] Universidad Tecnologica del Valle de Toluca, Carretera del Departamento del D.F. km. 7.5, Sta Maria Atarasquillo, CP 52044 Lerma, Mexico

[4] Laboratório de Nanotecnologia Fitofarmacêutica, Departamento de Ciências Biológicas e Saúde, Universidade Federal do Amapá (UNIFAP), Macapá AP, Brazil

[5] Laboratório de Farmacologia de Productos Naturales (LFPN), Facultat de Química, Universidad Nacional Autônoma de México (UNAM), Ciudad Universitária, 04510 México, DF, Mexico

[6] Laboratório de Química Farmacêutica e Medicinal (PharMedChem), Departamento de Ciências Biológicas e Saúde, Universidade Federal do Amapá (UNIFAP), Macapá, AP, Brazil

[7] Programa de Pós-Graduação em Inovação Farmacêutica, Curso de Farmácia, Departamento de Ciências Biológicas e Saúde, Universidade Federal do Amapá (UNIFAP), Macapá, AP, Brazil

Introduction

Nanotechnology is characterised by a multidisciplinary approach and involves the creation and usage of different systems nanometric proportions (De Villiers et al. 2009). Nanoformulations have a wide variety of applications (e.g. the food industry, cosmetics, medicines and pesticides) (Assis et al. 2012; Patel and Velikov 2011; Duncan 2011; Brumfiel 2006; Irache et al. 2011; Wang et al. 2007). Among nanoformulations, nanoemulsions are systems formed by two immiscible liquids and one or more stabilising liquids, which enable the formation of small droplets (McClements 2012).

Nanoemulsions are characterised by their thermodynamic stability and possess drop sizes between 20 and 200 nm (Ostertag et al. 2012). Those formulations have a wide variety of industrial applications (Izquierdo et al. 2002; Tadros et al. 2004) (e.g. as an adjuvant in foods, medicines and agricultural products), and they exhibit a high economic potential.

Essentials oils are complex mixtures of volatile substances extracted from plants. They typically contain monoterpenes, sesquiterpenes and other low molecular weight substances in addition to phenylpropanoids in some cases (plants used in drugs). The essentials oils are used in the food and pharmaceutical industries as flavouring agents and can be larval, antibacterial, antifungal, anticancer, antimutagenic, antidiabetic, antiviral, anti-inflammatory and antiprotozoal (Raut and Karuppayil 2010).

There is an active field research involving the anti-inflammatory drugs in nanoformulations. This field principally focuses on active compounds from natural products, which is the case for Z-ligustilide. This substance is isolated and purified from the essential oil of *Angelica sinensis*, and it attenuates inflammatory pain behaviour in mice (Kuang et al. 2006; Yu et al. 2008; Du et al. 2007).

Rosmarinus officinalis L. is a medicinal plant of the *Lamiaceae* family (Lorenzi and Matos 2002) that is commonly used for medicinal purposes. It is ingested as a tea (Marchiori 2004). This species is a copious producer of essential oils, and it has been studied thoroughly. It possesses several biological activities, including spasmolytic (Ventura-Martinez et al. 2011), antioxidant (Raškovic et al. 2014; Ojeda-Sana et al. 2013), antibacterial (Ojeda-Sana et al. 2013), anti-inflammatory (Melo et al. 2011), antidepressive (Machado et al. 2013) and antifungal (Gauch et al. 2014; Cleff et al. 2012) properties. The chemical composition of the essential oil of *Rosmarinus officinalis* L. (EORO) can vary according to several factors, such as climate, soil, sun exposure and extraction procedure. However, the chemotypes most commonly reported are cineoliferum, composed primarily of 1,8-cineole, and camphoric acid, where camphor prevails (Napoli et al. 2015).

EORO is mainly composed of terpenoids, more specifically monoterpenes. This group of terpenoids are biologically active, and many of these terpenoids possess anti-inflammatory activity (Souza et al. 2014). One of the components of this essential oil, 1,8-cineol/1,8-cineole/eucalyptol, had already been tested in a double-blind, placebo-controlled trial in patients with acute asthma and allergic inflammation. The results suggested that EORO exhibited anti-inflammatory activity in asthma and that it could be used as a mucolytic agent in upper and lower airway diseases (Juergens et al. 2003).

Here, we sought to obtain a nanoemulsion using EORO and to evaluate its anti-inflammatory potential in in vivo assays. We also evaluated the effects of the nanoemulsion on inflammation models and outlying pain in animals.

Methods and materials

EORO acquisition

We acquired the EORO from the Florien Company (Sao Paulo, Brazil). It had been botanically authenticated as being *Rosmarinus officinalis* L., and it possessed organoleptic, physicochemical and microbiological characteristics. It also contained essential oil from the rosemary plant, which was obtained from leaves collected in Brazil, lot 056757-LC02062016DA.

Analysis of EORO by GC–MS

Coupled gas chromatography–mass spectrometry (GC–MS) analyses were performed on a Shimadzu system/GC 2010 coupled to a self-gun Shimadzu/AOC-5000 and mass detector (Shimadzu MS2010 Plus) with electron impact (70 eV) equipped with a fused silica column of DB-5MS (Agilent Advanced J & W; 30 m × 0.25 mm × 0.25 μm). The parameters of the X were as follows: split ratio, 1:30; helium as the carrier gas (65 kPa); injection volume, 1.0 μl; injector temperature, 250 °C; detector temperature, 250 °C; initial column temperature, 60 °C for 1 min; heating rate, 3 °C min^{-1} to 290 °C. The total analysis time was 76.67 min, and we calculated retention indices (RI) via interpolation to the retention times for a mixture of aliphatic hydrocarbons (C9–C30) analysed under the same conditions. The MS fragmentation pattern of the compounds was also compared with NIST mass spectrum libraries (National Institute of Standards and Technology).

Nanoemulsion preparation

The nanoemulsions were prepared using a low-energy load methodology that has been described by Fernandes

et al. (2013). For a final mass of 50 g, we used 90% water, 5% EORO and 5% Tween 20. Initially, an organic phase was prepared by adding EORO and the tensioactive Tween into a beaker. The mixture was agitated using a magnetic agitator (750 rpm) for 30 min. Next, the aqueous phase was added at a flow rate of 0.5 mL/min with continuous agitation for 60 min. The stability of the emulsions was evaluated 1, 30 and 60 days after the preparation using macroscopic analysis (colour, visual aspect, phase separation, creaming and sedimentation) (Falcão et al. 2007). During this period, the emulsions were maintained at room temperature (25 ± 2 °C) in screw-capped glass test tubes.

Droplet size analysis

We determined droplet size and polydispersity with photon correlation spectroscopy using a Zetasizer 5000 (Malvern Instruments, Malvern, UK). Each emulsion was diluted using ultrapure Milli-Q water (1:25), and the measurements were performed in triplicate. The average droplet size was expressed as the mean diameter (Orafidiya and Oladimeji 2002).

Evaluation of EORO and NEORO on rat paw oedema, writhing test in mice and production of H_2S in rat stomachs

Experimental animals

Male Wistar rats (body weight: 180–200 g) were used, along with Swiss mice (body weight: 20–25 g) from the Central Biotério of the Department of Pharmacy of Faculdad de Química da Universidad Autonoma de Mexico. The animals were housed in polyethylene boxes in groups of five, and their access to food was removed 12 h prior to the experiments. They were given free access to water.

This research was approved by the Ethics Committee for the Use of Animals of Amapá Federal University (Authorisation No. 0021/2015). After the experiments, the animals were euthanised according to the guidelines for the euthanasia of animals (AVMA, American Veterinary Medical Association 2013).

Rat paw oedema induced by carrageenan

This test was carried out according to the method described by Winter et al. (1962). Groups of animals ($n = 5$) each received different doses of EORO (100 and 300 mg/kg) and NEORO (498 µg/kg) 30 min prior to the application of the inflammatory agent (carrageenan 1000 mg/paw, 01 mL, kappa, Sigma Company, Sao Paulo, Brazil). We administered 0.1 mL of saline solution in the plantar space of the left hind paw and the same volume containing the inflammatory agent in the right paw. We measured paw volume using a plethysmometer (Model 7540; Ugo Basile, Italy). The paws were measured every hour prior to the administration of the inflammatory substance and 4 h after the application of the carrageenan.

Acetic acid-induced writhing test

The acetic acid-induced writhing test was carried out in mice according to the method described by Koster et al. (1959). The different groups of animals were treated orally with EORO (100 mg/kg) and NEORO (166, 498 and 830 µg/kg), and the control animals were treated with 0.5 mL of Tween solution to 5%. Thirty minutes later, abdominal twitches (writhes) were induced intraperitoneally via (i.p.) administration of 1% acetic acid (0.25 mL). The writhing was observed, and we recorded the mean ± mean standard error of the number of writhes in an interval of 20 min.

Test of H_2S production in rat stomachs

This assay was based on the methods described by Khan et al. (1980) and Eto and Kimura (2002). Wistar rats were used ($n = 6$ per group), which were anaesthetised with sodium pentobarbital (10 mg/kg, i.p, Anestesal^{TM}, MSD, Mexico) and treated orally with EORO (100 mg/kg) and NEORO (498 µg/kg). After 30 min, L-cysteine was administered (100 mg/kg, via oral (v.o.), Sigma Company). The rats then underwent a laparotomy to reveal the pyloric region, and the H_2S microelectrodes were attached to an analyser system (Micro Hydrogen Sulfide Measurement System—microLazar Model ISM-146H2S-XS; Lazar, USA). We measured H_2S levels every 5 min, and after 30 min we injected 200 µL of ethyl alcohol (PA) directly in the animal's stomachs and recorded data for up to 60 min.

Molecular docking of the major chemical constituents of EORO

For the docking study, we downloaded files deposited in the Protein Data Bank (PDB) from the Research Collaboratory for Structural Bioinformatics (Li et al. 2007, 2008; Sandy and Butler 2009; Orlando and Malkowski 2016) with the coordinates of the crystallographic structures of the COX-1 therapeutic targets (PDB ID: 3N8X, resolution: 2.75 Å) complexed with the nimesulide inhibitor. COX-2 (PDB ID: 5IKQ, resolution: 2.41 Å) was complexed with meclofenamic acid and prostacyclin

(PDB ID: 3B6H, resolution: 2.41 Å) was complexed with the minoxidil inhibitor.

To perform the molecular docking, we added hydrogen atoms and removed water molecules from the enzymes. The inhibitors that were complexed with each therapeutic target were extracted. Prior to performing the docking simulation, we validated our results by calculating the root-mean-square deviation (RMSD) between the experimental binder and the conformation of the binder that yielded the best posture after docking. To calculate the docking of the major phytochemical constituents of EORO, we used the following coordinates: cyclooxygenase-1 (COX-1): x: −21.43, Y: −50.79 and z: 1.42; cyclooxygenase-2 (COX-2): Î½: 22.83, Y: 51.56 and z: 17.81; and prostacyclin (PGI-2): Î½: 72.25, Y: 54.20 and z: 42.19.

To identify the interactions between the compounds and the therapeutic targets, it was necessary to identify the amino acids that make up the catalytic site of the enzymes: COX-1 (ARG120, TYR355, SER530 and ILE523), COX-2 (TYR385 and SER530) and PGI-2 (CYS441, TRY282, PHE483 and GLY482).

Statistical analysis

We applied analysis of variance (ANOVA) followed by the Tukey test. *P* values less than 0.05 were considered to be statistically significant. We plotted the data using GraphPad Prism 6.0.

Results and discussion

The chromatographic data indicated that the EORO used in this study to obtain the NEORO contained the following major compounds: 21.99% limonene, 33.70% 1,8-cineole and 27.68% camphor (Fig. 1; Table 1). These results are in accordance with those reported by Zaouali et al. (2010). These authors found that camphor and 1,8-cineol were the primary compounds of EORO from Tunisia. In studies conducted by Boix et al. (2010) and Fernandes et al. (2013), α-pinene, 1,8-cineol and camphor were the primary components of EORO samples from Brazil. Ribeiro et al. (2012) found α-pinene and 1,8 cineol to be among the major compounds of EORO from fresh rosemary leaves cultivated in northeastern Brazil.

The nanoemulsion, NEORO, prepared with EORO, presented a fluid appearance, a whitish coloration and a slightly bluish reflection, which are common macroscopic characteristics in this type of formulation. The mean droplet diameter remained below 200 nm in all emulsions, as described by Solans et al. (2005) and Solè et al. (2012). As shown in Fig. 2, the NEORO presented a distribution of monomodal droplet sizes, but none of the samples exhibited signs of instability, such as cremation and phase separation, as described by Duarte et al. (2015).

The carrageenan-induced rat paw oedema assay is widely used as a test for evaluating anti-inflammatory activity. This assay has become a standard model for

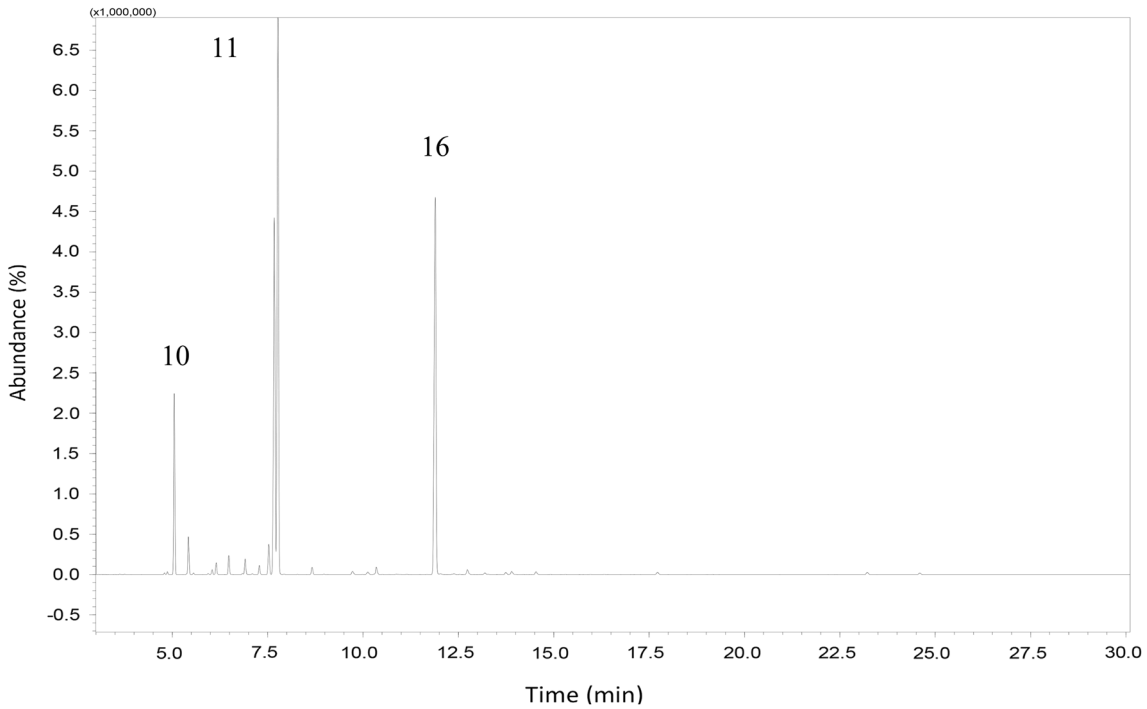

Fig. 1 Chromatogram obtained by analysis of EORO by coupled gas chromatography–mass spectrometry (GC–MS), where *10*—limonene (21.99%), *11*—1,8-cineole (33.70%) and *16*—camphor (27.68%)

Table 1 Chemical constituents of *Rosmarinus officinalis* L. essential oil (EORO) determined by GC–MS analysis

Peak	RT (min)	Compound	(%) GC–MS	RI experimental*	RI literature**
1	4.872	α-Thujene	0.11	928	926
2	5.054	α-Pinene	8.13	935	939
3	5.424	Camphene	1.68	950	954
4	6.045	β-Phellandrene	0.21	955	1031
5	6.152	β-Pinene	0.58	979	979
6	6.482	β-Myrcene	0.90	993	990
7	6.911	α-Phellandrene	0.77	1007	1002
8	7.282	α-Terpinene	0.45	1018	1017
9	7.532	o-Cymene	1.65	1026	1026
10	7.674	Limonene	21.99	1030	1031
11	7.773	1,8-Cineole	33.70	1033	1033
12	8.666	γ-Terpinene	0.39	1059	1059
13	9.724	Terpinolene	0.20	1091	1088
14	10.128	β-Linalool	0.16	1102	1098
15	10.350	***	0.44	1108	
16	11.897	Camphor	27.68	1147	1146
17	12.736	Borneol	0.32	1168	1169
18	13.739	α-Terpineol	0.12	1193	1188
19	13.899	α-Campholenal	0.20	1197	1125
20	14.532	Verbenone	0.18	1213	1205
21	23.220	β-Caryophyllene	0.12	1421	1427

* RI experimental: calculated RI

** RI literature: RI tabulated for compound

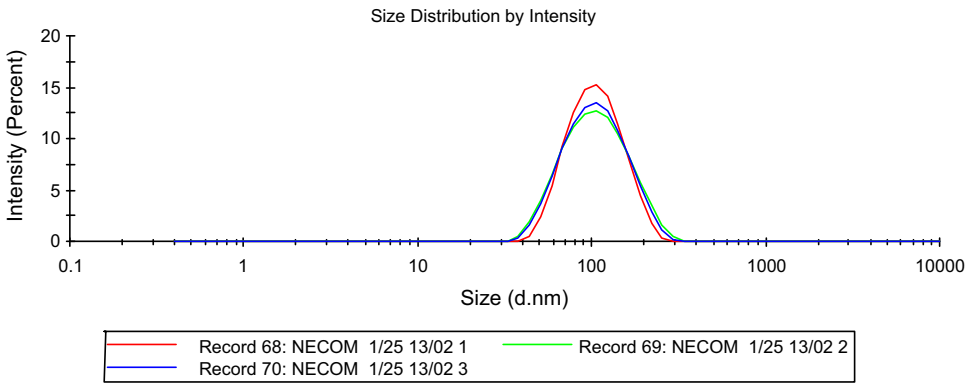

Fig. 2 Particle size distribution of NEORO mean droplet—89.87 ± 0,083727 nm; polydispersity 0.193 ± 0.008 nm

experiments related to acute inflammation, this is described as a biphasic response because it has an initial phase in the first 2 h after the injection of carrageenan, which is related to the release of histamine and serotonin and another phase that comprises the production of prostaglandins, bradykinin and proteases (Patgiri et al. 2014). Carrageenan was used in this assay because it is devoid of apparent systemic effects (Ganguly et al. 2013).

In a study by De Faria et al. (2011) focusing on EORO, the authors noted ED_{50} values of 300 and 261 mg/kg in the writhing test in mice and for carrageenan-induced paw oedema in rats, respectively. Additionally, LD_{50} in the mice was greater than 2.0 g/kg.

Oral administration of NEORO at a dose of 498 µg/kg inhibited the maximum peak of oedema by 46%, and EORO administered at a dose of 300 mg/kg inhibited the maximum peak of oedema by 50%. This result demonstrates that EORO delivered as a nanoemulsion was much more effective on carrageenan oedema, inhibiting this oedema, with a dose six hundred times lower than that of EORO (Fig. 3). In the acetic acid-induced writhing test in mice, the oral administration of NEORO yielded a dose-

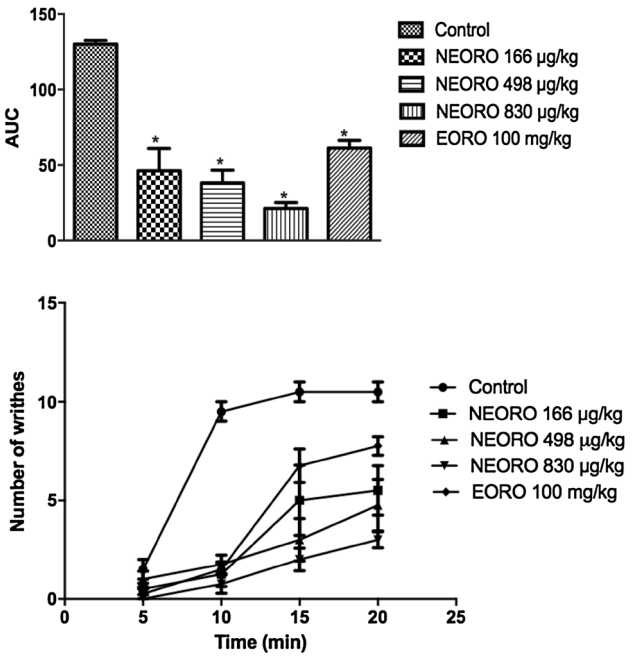

Fig. 3 Effect of oral treatments with EORO (100 mg/kg) and NEORO (166, 498 and 830 µg/kg) on writhing in mouse induced by acetic acid. The points represent the mean ± SEM of $n = 5$/group. $^*p < 0.05$, ANOVA followed by the Tukey test

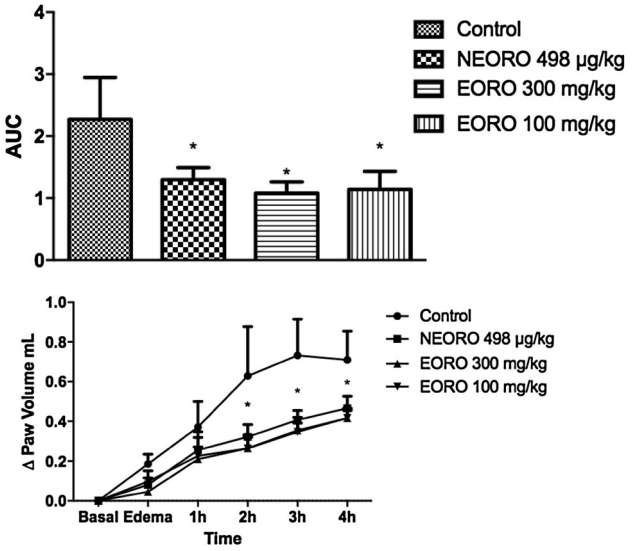

Fig. 4 Effect of oral treatments with EORO (100 and 300 mg/kg) and NEORO (498 µg/kg) on rat paw oedema induced by carrageenan. The points represent the mean ± SEM of $n = 5$/group. $^*p < 0.05$, ANOVA followed by the Tukey test

dependent effect, and a dose of 830 µg/kg inhibited the algogenic process by 84%. EORO alone at a dose of 100 mg/kg inhibited the algogenic process by 55% (Fig. 4).

The physiological functions of hydrogen sulphide (H_2S) have been recognised and evidence is being sought that this

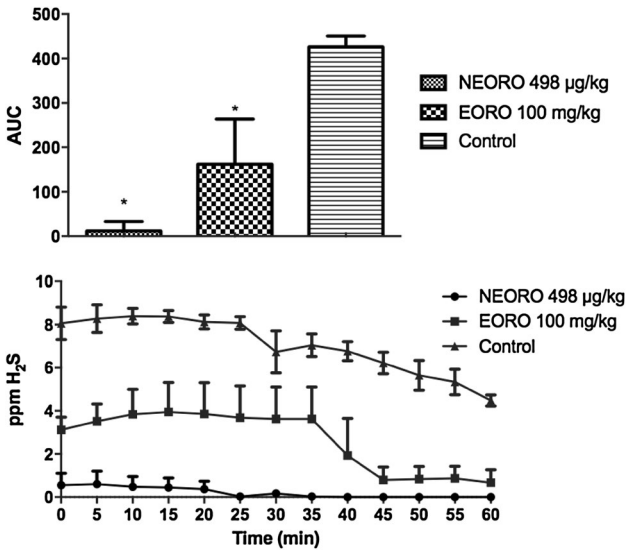

Fig. 5 Effect of oral treatments with EORO (100 mg/kg) and NEORO (498 µg/kg) on the production of H_2S in the stomach of Wistar rats. The points represent the mean ± SEM of $n = 5$/group. $^*p < 0.05$, ANOVA followed by the Tukey test

endogenous, gaseous substance can modulate inflammatory processes. However, H_2S donors have been shown to reduce oedema formation and the adhesion of leukocytes to vascular endothelium and inhibit the synthesis of proinflammatory cytokines (Wallace 2007). In addition, H_2S donors can increase gastric mucosal resistance to injury and accelerate repair (Wallace 2007). These observations and others suggest that anti-inflammatory drugs that are modified with the ability to release H_2S have improved anti-inflammatory efficacy and reduced toxicity (Wallace 2007).

In our analysis of how EORO and NEORO affected the L-cysteine-induced production of H_2S in rat stomachs, we observed that NEORO at a dose of 498 µg/kg inhibited production at all measurement times. Additionally, EORO at a dose of 100 mg/kg inhibited production of H_2S by 60% and potentiated the ethanol effect, thereby decreasing H_2S production (Fig. 5).

The evidence suggests that H_2S is a mediator of several aspects of the gastrointestinal function and liver. In addition, changes in H_2S production may contribute to diseases of the gastrointestinal tract and liver, and non-steroidal anti-inflammatory drugs may reduce the production of H_2S in the stomach, and this fact has been shown to contribute to the generation of mucosal injury (Fiorucci et al. 2005, 2006). However, Martínez et al. (2009) demonstrated the antinociceptive effect of EORO in arthritic pain in a rat model, suggesting the involvement of the serotonergic system via 5-HT_{1A} receptors and endogenous opioids. Furthermore, De Faria et al. (2011) described the anti-inflammatory effect of EORO via the inhibition of

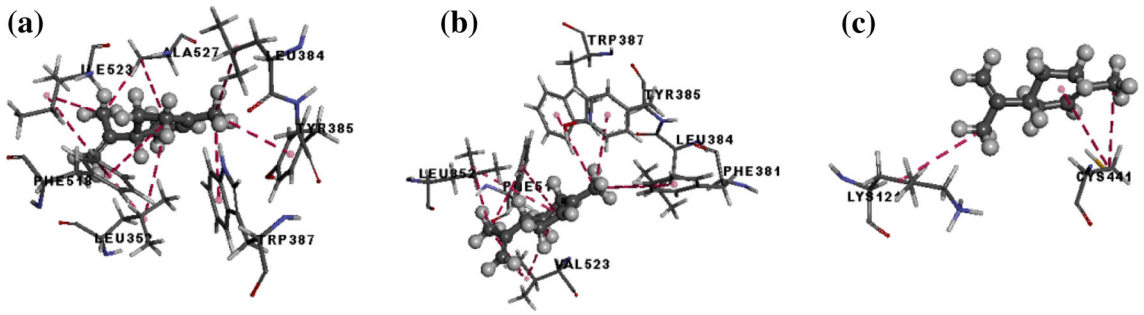

Fig. 6 Docking of the compound limonene performing interaction with **a** COX-1, **b** COX-2 and **c** PGI-2

cyclooxygenase; this effect persisted without causing gastric lesions or increasing mucus production. This fact may explain the observed results regarding H_2S production: a consistent mucus layer could interfere with the release of this mediator and, therefore, not be detected by the electrode system, a hypothesis that should be explored further in future studies.

Molecular docking is a computational method currently widely used in the drug discovery process (Chandak et al. 2014). The benefit of docking is to identify the mode of interaction of the study molecules at the site of the enzyme or receptor through specific key interactions and to predict the binding affinity between the protein-binding complexes, in this case, the chemical constituents of EORO. The Genetic Optimisation for Ligand Docking (GOLD) program uses a genetic algorithm to conduct flexible docking experiments of ligands within protein-binding sites. The GOLD program has been used to investigate the modes of interaction between compounds and therapeutic targets (Chandak et al. 2014).

The RMSD value indicates the accuracy of the docking postures calculated by the GOLD docking algorithm compared with the experimentally determined poses of a compound bound to a biological target. An RMSD less than 2 Å is considered to be successful (i.e. to have justified validity) (Cole et al. 2005). In this study, the best RMSD values obtained with nimesulide, meclofenamic acid and minoxidil inhibitors were 0.87, 0.99 and 0.89 Å for the respective therapeutic targets COX-1, COX-2 and PGI-2.

We then performed docking between the therapeutic targets and the compounds limonene, 1,8-cineole and camphor. We selected the docking results that yielded the highest score for each therapeutic target limonene: 50.14 for COX-1, 45.85 for COX-2 and 38.21 for PGI-2; 1,8-cineole compound: 36.30 for COX-1, 37.76 for COX-2 and 33.71 for PGI-2; camphor compound: 33.49 for COX-1, 34.38 for COX-2 and 36.13 for PGI-2.

With the COX-1 therapeutic target, the docking of the limonene compound had two alkyl-type hydrophobic interactions with distances of 3.97 and 4.22 Å from the amino acid ILE523 (Fig. 6a). Alkyl groups are defined as a predominantly aliphatic amino acid side chains, and they include alanine, valine, leucine, isoleucine, methionine, selenomethionine, cysteine, proline, CB, CG and CD atoms of lysine and CB and CG arginine atoms. Hydrophobic groups in binders are contiguous sets of atoms that are not adjacent to charge concentrations (charged atoms or electronegative atoms). A group of atoms is considered to be hydrophobic if its surface area is equal to or greater than the area of a methyl group multiplied by the surface area scale factor, which corresponds to the surface area of a chlorine atom. The criteria for this type of interaction were met when the centre of the groups was within 5.5 Å of an alkyl centre (Wolber and Langer 2005).

It is important to note that the limonene compound also exhibited numerous interactions with amino acids close to the amino acids of the active site of COX-1. Therefore, this compound can potentially modify the local structure, which can result in a biological effect. For the amino acid LEU352, we noted a hydrophobic interaction of the alkyl type with a distance of 5.13 Å. For the amino acid LEU384, we measured a hydrophobic interaction of the alkyl type with a distance of 4.91 Å. For the amino acid TYR385, we noted a hydrophobic interaction of the Pi–alkyl type with a distance of 4.21 Å. For the amino acid LEU387, we observed a hydrophobic P-alkyl-type interaction with a distance of 4.72 Å. For the amino acid PHE518, we observed two hydrophobic interactions, both of the Pi–alkyl type, with distances of 4.84 and 5.38 Å. For the amino acid ALA527, we noted two hydrophobic interactions of the alkyl type with distances of 3.75 and 4.78 Å.

For the COX-2 therapeutic target, the limonene compound presented a hydrophobic Pi–alkyl-like interaction with the amino acid residue TYR385 with a distance of 4.26 Å (Fig. 6b). Pi–sigma interactions are weak interactions between a hydrogen and a ring system Pi. Pi–alkyl interactions exist where the centres of an aromatic ring and an alkyl group are within the alkyl centroid limit with a

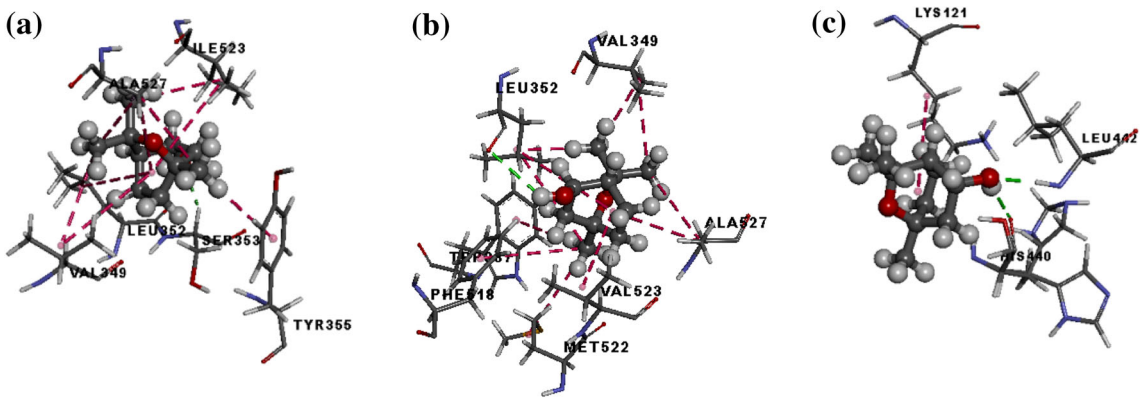

Fig. 7 Docking of the compound 1,8-cineole performing interaction with **a** COX-1, **b** COX-2 and **c** PGI-2

maximum distance of 5.5 Å, and they have at least one pair of atoms within the same atom closest to Pi–Pi. For this interaction to occur, the following conditions are necessary: (a) hydrogens that act as donors may be implicit or explicit hydrogens; they must be connected to a non-aromatic carbon atom; (b) the distances between the hydrogen and the centre of the Pi ring must be within a maximum distance of approximately 4.0 Å; (c) the centre angle CH can deviate from linear by a maximum of 20°; (d) the angle between the C-centre and the normal plane of the ring must not exceed 45° (Fares et al. 2016).

Among the amino acids close to the site of action of COX-2, the limonene compound had the following interactions: a hydrophobic Pi–alkyl-type interaction with the amino acid PHE381 with a distance of 5.27 Å, two hydrophobic interactions of the alkyl type with the amino acid LEU352 with distances of 3.90 and 5.19 Å were presented, a hydrophobic interaction of the alkyl type with the amino acid LEU384 with a distance of 4.48 Å, a hydrophobic interaction of the Pi–alkyl type with the amino acid TRP387 with a distance of 4.85 Å, two hydrophobic Pi–alkyl-type interactions with the amino acid PHE518 with distances of 4.87 and 5.31 Å, three hydrophobic interactions of the alkyl type with the amino acid VAL523 with distances of 3.92, 3.93 and 5.25 Å.

With the PGI-2 therapeutic target, the limonene compound exhibited two hydrophobic interactions with the amino acid CYS441 (both alkyl type with distances of 4.6 and 5.2 Å) (Fig. 1c). Regarding the amino acids close to the active site, the docking presented an alkyl-type hydrophobic interaction with a distance of 4.46 Å with the amino acid LYS121.

Regarding the therapeutic target COX-1, the 1,8-cineole compound exhibited hydrophobic binding of the Pi–alkyl type with the amino acid TYR355 with a distance of 4.46 Å. The 1,8-cineole compound also showed two hydrophobic bonds of the alkyl type with a distance of 5.37 Å and 4.43 Å with the amino acid ILE523 (Fig. 7).

Compound-1,8-cineole docking resulted in amino acid linkages very close to the amino acids of the active site of COX-1: two hydrophobic interactions with the amino acid LEU352 of the alkyl type at distances of 4.81 and 5.01 Å and a hydrogen bridge-type interaction with a distance of 2.28 Å. There were also two hydrophobic interactions with the amino acid VAL349 of the alkyl type with distances of 4.35 and 4.94 Å and four hydrophobic interactions with the amino acid ALA527 of the alkyl type with distances of 3.71, 3.94, 4.14 and 4.68 Å.

The docking of compound 1,8-cineole did not present interaction results with the amino acids present in the active site of the COX-2 and PGI-2 therapeutic targets. However, it presented interactions with seven amino acids close to the active site of COX-2 and interactions with three amino acids close to the active site of PGE2.

In terms of the amino acids close to the active site of COX-2, the docking exhibited two hydrophobic alkyl-type interactions with the amino acid VAL349 with distances of 4.51 and 4.01 Å; three hydrophobic interactions of the alkyl type with the amino acid LEU352 with distances of 5.40, 5.21 and 3.61 Å; and a conventional hydrogen-bonding interaction with a distance of 2.93 Å.

The amino acids close to the active site of PGI-2 that showed an interaction included LYS121 (with a hydrophobic interaction of alkyl type with a distance of 5.17 Å), the amino acid HIS440, which exhibited a hydrogen-bonding interaction of the conventional type with a distance of 2.14 Å, and the amino acid LEU442 interaction of a conventional-type hydrogen bridge with a distance of 1.90 Å.

The compound that exhibited the largest number of interactions with the therapeutic targets was camphor. In the COX-1 therapeutic target, this compound exhibited an

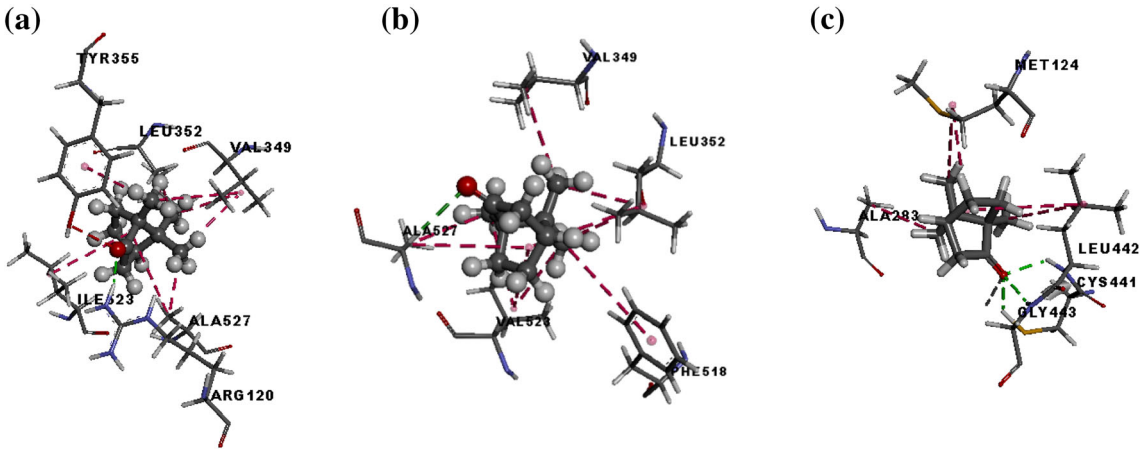

Fig. 8 Docking of the camphor compound performing interaction with nearby amino acids and of the active site of COX-1, COX-2 and PGI-2

interaction of conventional hydrogen bonds with the ARG120 amino acid with a distance of 2.10 Å. Conventional hydrogen-bonding interactions may exist between a hydrogen-bonding donor atom and an acceptor atom such as N, O, P or S. The maximum accepted distance for this bond is 3.8 Å (Bissantz et al. 2010; Ziólkowski et al. 2006). For the same target, a hydrophobic interaction with the amino acid ILE523 of the alkyl type with a distance of 4.52 Å was presented. We also noted a hydrophobic interaction of the Pi–alkyl type with a distance of 4.36 Å with the amino acid TRY355 (Fig. 8a).

With the amino acids present near the active site of COX-1, the docking presented three hydrophobic alkyl-type interactions with distances of 3.76, 4.18 and 4.80 Å with the amino acid VAL349; two hydrophobic interactions of the alkyl type with distances of 3.47 and 4.65 Å with the amino acid LEU352; and two hydrophobic alkyl-type interactions with distances of 3.33 Å and 4.94 Å with the amino acid ALA527 (Table 2).

In terms of the docking of the compound camphor with COX-2, this did not present interaction results with the amino acids present in the site. However, camphor presented interactions with amino acids close to the active site: an alkyl-type hydrophobic interaction with a distance of 4.16 Å with the amino acid VAL349; three hydrophobic alkyl-type interactions with distances of 3.66, 4.08 and 4.64 Å with the amino acid LEU352; a hydrophobic interaction of the Pi–alkyl type with a distance of 5.41 Å with the amino acid PHE518; three hydrophobic interactions of the alkyl type with distances of 3.84, 4.30 and 4.41 Å with the amino acid VAL523; two alkyl-type hydrophobic interactions with distances of 4.81 and 3.65 Å; and a hydrogen-bonding interaction with the amino acid ALA527.

Camphor docking with the therapeutic target PGI-2 yielded two hydrogen-bonding interactions: a conventional interaction with a distance of 2.09 Å and a carbon–hydrogen-type interaction with a distance of 2.09 Å. Both interactions occurred at amino acid CYS441 (Fig. 8b).

The docking results yielded the following interactions with the amino acids close to the active site: two hydrophobic alkyl-type interactions with the amino acid MET124 with distances of 4.93 and 4.95 Å; a hydrophobic alkyl-type interaction with a distance of 4.15 Å with the amino acid ALA283; an alkyl-type hydrophobic interaction with a distance of 5.07 Å; a conventional hydrogen-bonding interaction with a distance of 4.72 Å with the amino acid LEU 442; a conventional hydrogen-bonding interaction with the amino acid GLY 443 with a distance of 2.08 Å; and a metal–receptor type interaction with a distance of 2.61 Å (Fig. 8c).

Conclusion

Our results demonstrate the importance of nanotechnology as an alternative for the delivery of drugs. Nanotechnology is capable of increasing the bioavailability of active principles from vegetable drugs and improving its action on certain target systems. The nanoemulsion (NEORO) obtained from EORO was able to reduce rat paw oedema induced by carrageenan with a dose 600 times lower than the effective dose of EORO, and it produced a dose–response effect in the algesic test. NEORO accordingly demonstrated a potent antialgic effect. With the results obtained in the molecular docking study, we observed that among the primary compounds of EORO the camphor molecule presented the largest number of interactions with therapeutic targets related to the inflammatory process. This finding suggests that the camphor molecule is responsible for the anti-inflammatory and antialgic effects observed in the experimental results with NEORO and

Table 2 Interactions between amino acids nearby and of the active site of the biological target and distances where interactions occur

Compounds of EORO	Active site amino acids	Atoms involved	Type of interaction	Distance (Å)
Limonene	COX-1			
	ILE523	C9—CG1	Hydrophobic	3.97
		C10—CG1	Hydrophobic	4.22
	LEU352	Cyclohexane—CG	Hydrophobic	5.13
	LEU384	C8—aromatic ring	Hydrophobic	4.91
	TYR385	C8—aromatic ring	Hydrophobic	4.21
	LEU387	C8—aromatic ring	Hydrophobic	4.72
	PHE518	C10—aromatic ring	Hydrophobic	4.84
		Cyclohexane—aromatic rings	Hydrophobic	5.38
	ALA527	C9—CB	Hydrophobic	3.75
		Cyclohexane—CB	Hydrophobic	4.78
	COX-2			
	TYR385	C8—aromatic ring	Hydrophobic	4.26
	PHE381	C8—aromatic ring	Hydrophobic	5.27
	LEU352	C9—aromatic ring	Hydrophobic	3.90
		Cyclohexane—CG	Hydrophobic	5.19
	LEU384	C8—CG	Hydrophobic	4.48
	TRP387	C9—aromatic ring	Hydrophobic	4.85
	PHE518	Cyclohexane—CG	Hydrophobic	4.87
			Hydrophobic	5.31
	VAL523	C9—CG2	Hydrophobic	3.92
		C10—CG1	Hydrophobic	3.93
		Cyclohexane—CG1	Hydrophobic	5.25
	PGI-2			
	CYS441	C8—SG	Hydrophobic	4.60
		Cyclohexane—SG	Hydrophobic	5.20
	LYS121	C9—CG	Hydrophobic	4.46
1,8-Cineole	COX-1			
	TYR355	C10—aromatic ring	Hydrophobic	4.46
	ILE523	C12—CG1	Hydrophobic	5.37
		H21—CG1	Hydrophobic	4.43
	LEU352	C11—CG	Hydrophobic	4.81
		C4—CG	Hydrophobic	5.01
	VAL349	C11—CG2	Hydrophobic	4.35
		C6—CG2	Hydrophobic	4.94
	ALA527	C12—CB	Hydrophobic	3.71
		C11—CB	Hydrophobic	3.94
		C10—CB	Hydrophobic	4.14
		C6—CB	Hydrophobic	4.68
	COX-2			
	VAL349	C11—CB	Hydrophobic	4.01
		C12—CB	Hydrophobic	3.51
	LEU352	C12—CG	Hydrophobic	5.40
		Cyclohexane—CD2	Hydrophobic	5.21
		H28—CG	Hydrophobic	3.60
		H15—O	Conventional H bond	2.93
	PGI-2			
	LYS121	Cyclohexane—CG	Hydrophobic	5.17
	HIS440	H15—O	Conventional H bond	2.14
	LEU442	O2—H	Conventional H bond	1.90

Table 2 continued

Compounds of EORO	Active site amino acids	Atoms involved	Type of interaction	Distance (Å)
Camphor	COX-1			
	ARG120	01—H22	Conventional H bond	2.10
	TYR355	H25—aromatic ring	Hydrophobic	4.36
	ILE523	Cyclohexane—HB	Hydrophobic	4.52
	VAL349	C9—CB	Hydrophobic	3.76
		C10—CB	Hydrophobic	4.18
		C11—CB	Hydrophobic	4.80
	LEU352	C9—CG	Hydrophobic	3.47
		Cyclohexane—CG	Hydrophobic	4.65
	ALA527	C10—CB	Hydrophobic	3.33
		Cyclohexane—CB	Hydrophobic	4.94
	COX-2			
	VAL349	H23—CB	Hydrophobic	4.16
	LEU352	C10—CG	Hydrophobic	3.66
		C9—CG	Hydrophobic	4.08
		Cyclohexane—CG	Hydrophobic	4.64
	PHE518	C9—aromatic ring	Hydrophobic	5.41
	VAL523	C9—CB	Hydrophobic	3.84
		C11—CB	Hydrophobic	4.30
		Cyclohexane—CB	Hydrophobic	4.41
	ALA527	Cyclohexane—CB	Hydrophobic	4.81
		C11—CB	Hydrophobic	3.65
		O1—HA	Conventional H bond	2.58
	PGI-2			
	CYS441	O1—HG	Conventional H bond	2.09
		O1—HA	Carbon H bond	2.09
	MET124	Cyclohexane—SD	Hydrophobic	4.93
		C9—SD	Hydrophobic	4.95
	ALA283	C10—CB	Hydrophobic	4.15
	LEU442	Cyclohexane—CG	Hydrophobic	5.07
		O1—H	Conventional H bond	4.72
	GLY443	O1—H	Conventional H bond	2.08

EORO. However, additional studies are necessary to elucidate the mechanism of H_2S production.

Acknowledgements The authors acknowledge PNPD/CAPES (Program/Project: PNPD20130076-14001012005P1), CAPES (No. 3292/2013 AUXPE) and CNPq Proc. 402332/2013-0 for financial support and the Universidad Autônoma de México—Programa de Estancias de Investigación (PREI).

References

American Veterinary Medical Association (2013) Guidelines for the Euthanasia of Animals: 2013 Edition. 48–50

Assis LM, Zavareze ER, Prentice-Hernández C, Souza-Soares LA (2012) Characteristics of nanoparticles and their potential applications in foods. Braz J Food Technol 15:99–109

Bissantz C, Kuhn B, Stahl M (2010) A medicinal chemist's guide to molecular interactions. J Med Chem 53(14):5061–5084

Boix YF, Victório CP, Lage CLS, Kuster RM (2010) Volatile compounds from *Rosmarinus officinalis* L. and *Baccharis dracunculifolia* DC. Growing in southeast coast of Brazil. Quím Nova 33:255–257

Brumfiel G (2006) Consumer products leap aboard the nano bandwagon. Nature 440:262

Chandak N, Kumar P, Kaushik P, Varshney P, Sharma C, Kaushik D, Jain S, Aneja KR, Sharma PK (2014) Dual evaluation of some novel 2-amino-substituted coumarinylthiazoles as anti-inflammatory–antimicrobial agents and their docking studies with COX-1/COX-2 active sites. J Enzym Inhib Med Chem 29:476–484

Cleff MB, Meinerz ARM, Madrid I, Fonseca AO, Alves GH, Meireles MCA, Rodrigues MRA (2012) Perfil de suscetibilidade de leveduras do gênero Candida isoladas de animais ao óleo essencial de *Rosmarinus officinalis* L. Rev Bras Planta Med Botucatu 14(1):43–49

Cole JC, Nissink JWM, Taylor R (2005) Protein-ligand docking and virtual screening with GOLD. In: Alvarez J, Shoichet B (eds) Virtual Screening in Drug Discovery. CRC Press, Boca Raton, Fla, pp 379–415

De Faria LRD, Lima CS, Perazzo FF, Carvalho JCT (2011) Anti-inflammatory and antinociceptive activities of the essential oil from *Rosmarinus officinalis* L. (Lamiaceae). Int J Pharm Sci Rev Res 7:2

De Villiers MN, Aramwit P, Kwon GS (eds) (2009) Nanotechnology in drug delivery. Springer & AAPS Press, NY, p 663p

Du J, Yu Y, Ke Y, Wang C, Zhu L, Qian ZM (2007) Ligustilide attenuates pain behavior induced by acetic acid or formalin. J Ethnopharmacol 112:211–214

Duarte JL, Amado JRR, Oliveira AEMFM, Cruz RAS, Ferreira AM, Souto RNP, Falcão DQ, Carvalho JCT, Fernandes CP (2015) Evaluation of larvicidal activity of a nanoemulsion of *Rosmarinus officinalis* essential oil. Rev Bras Farmacogn 25:189–189

Duncan TV (2011) Applications of nanotechnology in food packaging and food safety: barrier materials, antimicrobials and sensors. J Colloid Interface Sci 363:1–24

Eto K, Kimura H (2002) A novel enhancing mechanism for hydrogen sulfide-producing activity of cystathionine beta-synthase. J Biol Chem 277:42680–42685

Falcão AP, Chaves ES, Kuskoski EM, Fett R, Falcão DL, Bordignon-Luiz T (2007) Índice de polifenóis, antocianinas totais e atividade antioxidante de um sistema modelo de geléia de uvas. Ciênc Tecnol Aliment 27:637–642

Fares M, Said MA, Alsherbiny MA, Eladwy RA, Almahli H, Abdel-Aziz MM, Ghabbour HA, Eldehna WM, Abdel-Aziz HA (2016) Synthesis, biological evaluation and molecular docking of certain sulfones as potential nonazole antifungal agents. Molecules 21:1–16

Fernandes CP, Mascarenhas MP, Zibetti FM, Lima BG, Oliveira RPRF, Rocha L, Falcão DQ (2013) HLB value, an important parameter for the development of essential oil phytopharmaceuticals. Braz J Pharm 23(1):108–114

Fiorucci S, Antonelli E, Distrutti E, Rizzo G, Mencarelli A, Orlandi S, Zanardo R, Renga B, Di Sante M, Morelli A, Cirino G, Wallace JL (2005) Inhibition of hydrogen sulfide generation contributes to gastric injury caused by anti-inflammatory nonsteroidal drugs. Gastroenterology 129(4):1210–1224

Fiorucci S, Distrutti E, Cirino G, Wallace JL (2006) The emerging roles of hydrogen sulfide in the gastrointestinal tract and liver. Gastroenterology 131:259–271

Ganguly A, Al Mahmud Z, Muhammad Nasir Uddin M, Abdur Rahman SM (2013) In-vivo anti-inflammatory and anti-pyretic activities of Manilkara zapota leaves in albino Wistar rats. Asian Pac J Trop Dis 3(4):301–307

Gauch LMR, Silveira-Gomes F, Esteves RA, Pedrosa SS, Gurgel ESC, Arruda AC, Marques-Da-Silva SH (2014) Effects of *Rosmarinus officinalis* essential oil on germ tube formation by *Candida albicans* isolated from denture wearers. Rev Soc Brasil Med Trop 47(3):389–391

Irache JM, Esparza I, Gamazo C, Agüeros M, Espuelas S (2011) Nanomedicine: novel approaches in human and veterinary therapeutics. Vet Parasitol 180:47–71

Izquierdo P, Esquena J, Tadros TF, Dederen C, Garcia MJ, Azemar N, Solans C (2002) Formation and stability of nano-emulsions prepared using the phase inversion temperature method. Langmuir 18:26–30

Juerges UR, Dethlefsen U, Steinkamp G, Gillissen A, Repges R, Vetter H (2003) Anti-inflammatory activity of 1.8-cineol (eucalyptol) in bronchial asthma: a double-blind placebo-controlled trial. Respir Med 97:250–256

Khan SU, Morris GF, Hidiroglou M (1980) Rapid estimation of sulfide in rumen and blood with a sulfide-specific ion electrode. Microchem J 25:388–395

Koster R, Anderson M, De Beer EJ (1959) Acetic acid for analgesic screening. Fed Proc 18:412–418

Kuang X, Yao Y, Du JR, Liu YX, Wang CY, Qian ZM (2006) Neuroprotective role of Z-ligustilide against forebrain ischemic injury in ICR mice. Brain Res 1102:145–153

Li L, Rossoni G, Sparatore A, Lee LC, Del Soldato P, Moore PK (2007) Anti-inflammatory and gastrointestinal effects of a novel diclofenac derivative. Free Radic Biol Med 42:706–719

Li YC, Chiang CW, Yeh HC, Hsu PY, Whitby FG, Wang LH, Chan NL (2008) Structures of prostacyclin synthase and its complexes with substrate analog and inhibitor reveal a ligand-specific heme conformation change. J Biol Chem 283:2917–2926

Lorenzi HE, Matos FJA (2002) Plantas medicinais no Brasil: Nativas e exóticas. Instituto Plantarum de Estudos de Flora, Nova Odessa, p 512

Machado DG, Cunha MP, Neis VB, Balen GO, Colla A, Bettio LEB, Oliveira A, Pazini FL, Dalmarco JB, Simionatto EL, Pizzolatti MG, Rodrigues ALS (2013) Antidepressant-like effects of fractions, essential oil, carnosol and betulinic acid isolated from *Rosmarinus officinalis* L. Food Chem 136:999–1005

Marchiori VF (2004) *Rosmarinus officinalis.* Monografia (Curso de Fitomedicina). Associação Argentina de Fitomedicina, Argentina, Fundação Herbarium, p 32

Martínez AL, González-Trujano ME, Pellicer F, López-Muñoz FJ, Navarrete A (2009) Antinociceptive effect and GC/MS analysis of *Rosmarinus officinalis* L. essential oil from its Aerial parts. Planta Med 75:508–511

McClements DJ (2012) Nanoemulsions versus microemulsions: terminology, differences, and similarities. Soft Matter 8:1719–1729

Melo GAN, Grespan R, Fonseca JP, Farinha TO, Silva EL, Romero AL, Bersani A, Cuman RK (2011) *Rosmarinus officinalis* L. essential oil inhibits in vivo and in vitro leukocyte migration. J Med Food 14(9):944–949

Napoli EM, Siracusa L, Saija A, Speciale A, Trombetta D, Tuttolomondo T, La Bella S, Licata M, Virga G, Leone R, Leto C, Rubino L, Ruberto G (2015) Wild Sicilian rosemary: phytochemical and morphological screening and antioxidant activity evaluation of extracts and essential oils. Chem Biodivers 12:1075–1094

Ojeda-Sana AM, Van Baren CM, Elechosa MA, Juarez MA, Moreno S (2013) New insights into antibacterial and antioxidant activities of Rosemary essential oil and their main components. Food Control 31:189–195

Orafidiya LO, Oladimeji FA (2002) Determination of the required HLB values of some essential oils. Int J Pharm 237:241–249

Orlando BJ, Malkowski MG (2016) Substrate-selective inhibition of cyclooxygenase-2 by fenamic acid derivatives is dependent on peroxide tone. J Biol Chem 291:15069–15081

Ostertag F, Weiss J, McClements DJ (2012) Low-energy formation of edible nanoemulsions: factors influencing droplet size produced by emulsion phase inversion. J Colloid Interface Sci 388:95–112

Patel AR, Velikov KP (2011) Colloidal delivery systems in foods: a general comparison with oral drug delivery LWT. Food Sci Technol 44:1958–1964

Patgiri B, Umretia BL, Vaishnav PU, Prajapati PK, Shukla VJ, Ravishankar B (2014) Anti-inflammatory activity of Guduchi Ghana (aqueous extract of *Tinospora cordifolia* Miers.). Int Q J Res Ayurveda 35:108–110

Rašković A, Milanović I, Pavlović N, Ćebović T, Vukmirović S, Mikov M (2014) Antioxidant activity of rosemary (*Rosmarinus officinalis* L.) essential oil and its hepatoprotective potential. BMC Complement Altern Med 14:225

Raut JS, Karuppayil SM (2010) A status on the medicinal properties of essential oils. Ind Crops Products 62:250–264

Ribeiro DS, Melo DB, Guimarães AG, Velozo ES (2012) Avaliação do óleo essencial de alecrim (*Rosmarinus officinalis* L.) como

modulador da resistência bacteriana. Semina: Ciências Agrárias 33:687–696

Sandy M, Butler A (2009) Microbial Iron Acquisition: marine and Terrestrial Siderophores. Chem Rev 109:4580–4595

Solans C, Izquierdo P, Nolla J, Azemar N, Garcia-Celma MJ (2005) Nano-emulsions. Curr Opin Colloid Interface Sci 10:102–110

Solè I, Solans C, Maestro A, González C, Gutiérrez JM (2012) Study of nano-emulsion formation by dilution of microemulsions. J Colloid Interface Sci 376:133–139

Souza MT, Almeida JR, Araujo AA, Duarte MC, Gelain DP, Moreira JC, dos Santos MR, Quintas-Júnior LJ (2014) Structure–activity relationship of terpenes with anti-inflammatory profile—a systematic review. Basic Clin Pharmacol Toxicol 115:244–256

Tadros T, Izquierdo P, Esquena J, Solans C (2004) Formation and stability of nano-emulsions. Adv Colloid Interface Sci 108–109:303–318

Ventura-Martinez R, Rivero-Osorno O, Gómez C, González-Trujano ME (2011) Spasmolytic activity of *Rosmarinus officinalis* L. involves calcium channels in the guinea pig ileum. J Ethnopharmacol 137:1528–1532

Wallace JL (2007) Hydrogen sulfide-releasing anti-inflammatory drugs. Trends Pharmacol Sci 28:10

Wang L, Li X, Zhang G, Dong J, Eastoe J (2007) Oil-in-water nanoemulsions for pesticide formulations. J Colloid Interface Sci 314:230–235

Winter CA, Risley EA, Nuss GW (1962) Carrageenin-induced edema in hind paw of the rat as an assay for anti-inflammatory drugs. Proc Soci Exp Biol Med 111:544–547

Wolber G, Langer T (2005) LigandScout: 3-D pharmacophores derived from protein-bound ligands and their use as virtual screening filters. J Chem Inf Model 45:160–169

Yu Y, Du JR, Wang CY, Qian ZM (2008) Protection against hydrogen peroxide-induced injury by Z-ligustilide in PC12 cells. Exp Brain Res 184(3):307–312

Zaouali Y, Bouzaine T, Boussaid M (2010) Essential oils composition in two *Rosmarinus officinalis* L. varieties and incidence for antimicrobial and antioxidant activities. Food Chem Toxicol 48:3144–3152

Ziólkowski M, Grabowski SJ, Leszczynski J (2006) Cooperativity in hydrogen-bonded interactions: Ab initio and "atoms in molecules" analyses. J Phys Chem A 110(20):6514–6521